



ELSEVIER

Thermochimica Acta 339 (1999) 95–101

thermochimica  
acta

www.elsevier.com/locate/tca

# Studies of the thermal decomposition of (2-thiazolin-2-yl)hydrazine hydrochloride and some metal derivative complexes

A. Bernalte-García<sup>a</sup>, F.J. García-Barros<sup>a</sup>, F.J. Higes-Rolando<sup>a,\*</sup>,  
A.M. Pizarro-Galán<sup>a</sup>, C. Valenzuela-Calahorra<sup>b</sup>

<sup>a</sup>Departamento de Química Inorgánica, Facultad de Ciencias, Universidad de Extremadura, 06071 Badajoz, Spain

<sup>b</sup>Departamento de Química Inorgánica, Facultad de Farmacia, Universidad de Granada, 18071 Granada, Spain

Received 9 February 1999; received in revised form 7 July 1999; accepted 9 July 1999

## Abstract

The compound (2-thiazolin-2-yl)hydrazine hydrochloride (TzHyHCl) and the complexes  $[\text{Ni}(\text{TzHy})_2(\text{H}_2\text{O})_2]\text{Cl}_2 \cdot 2\text{H}_2\text{O}$ ,  $[\text{ZnCl}(\text{TzHy})_2]\text{Cl}$  and  $[\text{Cd}(\text{TzHy})(\mu\text{-Cl})_2]_n \cdot n\text{H}_2\text{O}$  have been studied using spectral (IR and electronic) and thermal (TG and DSC) methods. © 1999 Published by Elsevier Science B.V. All rights reserved.

**Keywords:** Hydrazine; Thiazoline; DSC; TG; Spectroscopic studies

## 1. Introduction

Some compounds structurally similar to (2-thiazolin-2-yl)hydrazine hydrochloride (TzHyHCl), such as 2-amino-2-thiazoline hydrochloride, have been used in clinical trials where they have shown therapeutical action since they are able to induce the “reverse transformation” in tumor cells [1,2].

As part of our program on the coordination chemistry of TzHyHCl we have reported its coordination behaviour and equilibria study with nickel(II), zinc(II) and cadmium(II) in aqueous solution. Likewise, the solid phases obtained by the reaction between the ligand and the aforementioned divalent cations have been characterized by elemental analysis and X-ray diffraction. These phases are  $[\text{Ni}(\text{TzHy})_2(\text{H}_2\text{O})_2]\text{Cl}_2 \cdot 2\text{H}_2\text{O}$ ,  $[\text{ZnCl}(\text{TzHy})_2]\text{Cl}$  and  $[\text{Cd}(\text{TzHy})(\mu\text{-Cl})_2]_n \cdot n\text{H}_2\text{O}$  [3,4].

In this paper we report the thermal behaviour and the IR spectra of TzHyHCl and the mentioned complexes, so as the electronic spectrum of the nickel(II) complex.

## 2. Experimental

The compound TzHyHCl and its nickel(II), zinc(II) and cadmium(II) complexes were prepared according to a reported procedure [3,4].

### 2.1. Apparatus and measurements

Thermal studies were carried out on a Mettler MTA 3000 system provided with a Mettler TG 50 thermobalance and a Mettler DSC-20 differential scanning calorimeter. The TG–DTG curves were obtained in a dynamic air atmosphere (flow rate,  $200 \text{ ml min}^{-1}$ ) in a

\*Corresponding author

temperature range of 30–900°C with sample masses between 10 and 15 mg and a heating rate of 10°C min<sup>-1</sup>.

The DSC curves were recorded at a heating rate of 10°C min<sup>-1</sup> in a temperature range of 30–600°C using sample masses around 3 mg.

Infrared spectra were recorded as KBr discs using a Perkin-Elmer FT-IR 1720 spectrophotometer in the 4000–400 cm<sup>-1</sup> region and as polyethylene plates on a Perkin-Elmer FT-IR 1700X spectrophotometer in the 400–150 cm<sup>-1</sup> region.

A UV–vis–NIR reflectance spectrum of the nickel(II) complex in the 220–1000 nm range was obtained from a pellet of the sample using a Shimadzu UV-3101PC spectrophotometer and BaSO<sub>4</sub> as a reference.

X-ray powder diffraction patterns were obtained through a Philips PW-1700 diffractometer using CuK<sub>α</sub> radiation ( $\lambda = 1.5406 \text{ \AA}$ )

### 3. Results and discussion

#### 3.1. Thermal study

TG–DTG and DSC curves for TzHyHCl and the complexes are shown in Figs. 1 and 2, respectively.

##### 3.1.1. TzHyHCl

The first effect observed in the DSC curve is a sharp endothermic peak at 200°C. This effect is not associated with a mass change in the TG–DTG curve, and

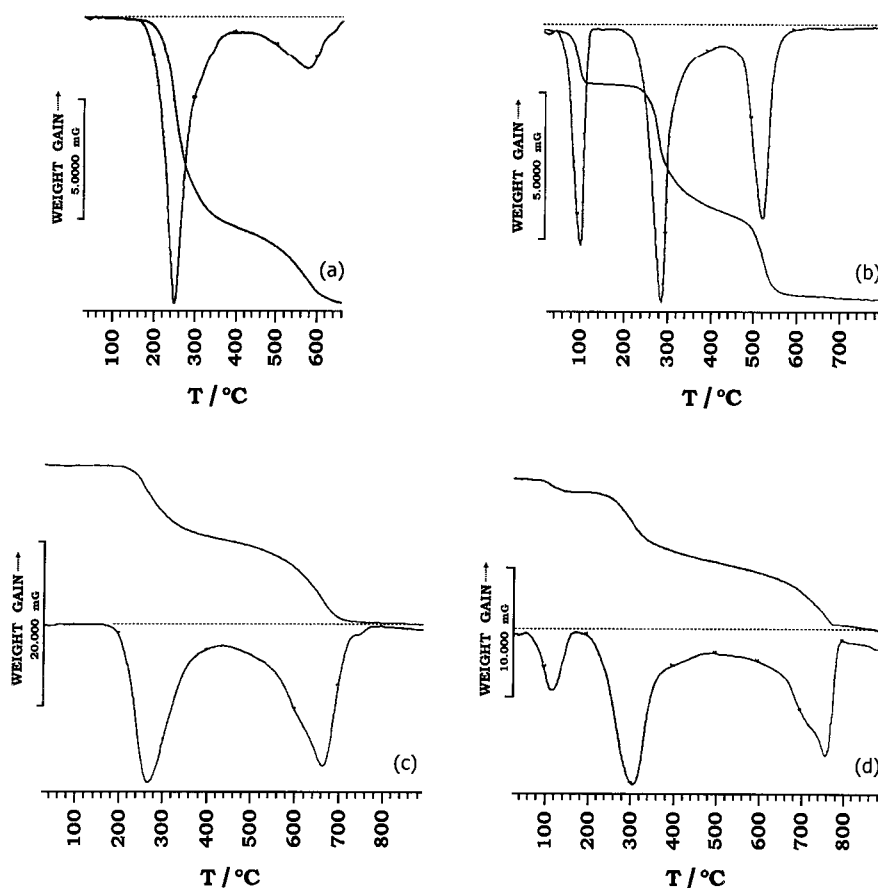


Fig. 1. TG–DTG curves for: (a) TzHyHCl; (b) [Ni(TzHy)<sub>2</sub>(H<sub>2</sub>O)<sub>2</sub>]Cl<sub>2</sub>·2H<sub>2</sub>O; (c) [ZnCl(TzHy)<sub>2</sub>]Cl; and (d) [Cd(TzHy)(μ-Cl)<sub>2</sub>]<sub>n</sub>·nH<sub>2</sub>O.

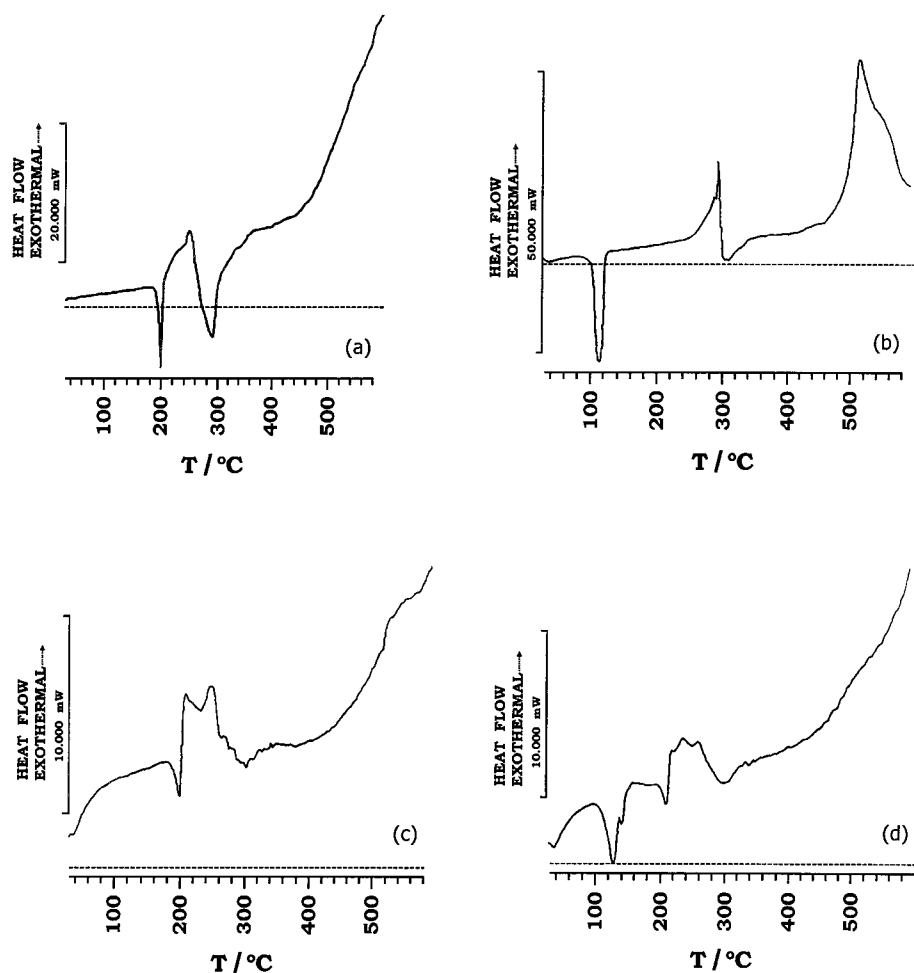


Fig. 2. DSC curves for: (a) TzHyHCl; (b)  $[\text{Ni}(\text{TzHy})_2(\text{H}_2\text{O})_2]\text{Cl}_2 \cdot 2\text{H}_2\text{O}$ ; (c)  $[\text{ZnCl}(\text{TzHy})_2]\text{Cl}$ ; and (d)  $[\text{Cd}(\text{TzHy})(\mu\text{-Cl})_2]_n \cdot n\text{H}_2\text{O}$ .

can be attributed to the fusion of ligand. The calculated enthalpy for this process is 153 J/g.

The DSC curve shows a second endothermic effect in the range 260–390°C which corresponds to a strong mass loss (75.8%) in the TG–DTG curve. This effect is assigned to pyrolysis of ligand.

At temperature over 400°C a third exothermic effect appears in the TG–DTG curve which can be assigned to the total combustion of the carbonaceous residue proceeding from the pyrolysis.

### 3.1.2. $[\text{Ni}(\text{TzHy})_2(\text{H}_2\text{O})_2]\text{Cl}_2 \cdot 2\text{H}_2\text{O}$

The TG–DTG curve of the nickel(II) complex shows a mass loss between 50°C and 140°C corresponding to the liberation of four moles of water per

mole of complex (obs.: 16.6%; calc.: 16.5%). The expected endothermic behaviour of this process ( $\Delta H = 523 \text{ J/g}$ ) appears in the DSC curve in the same temperature range.

Between 250°C and 350°C, the DSC curve displays two overlapping effects. The first is exothermic and the second is endothermic. The calculated enthalpies to the change of effect are  $-292 \text{ J/g}$  and  $123 \text{ J/g}$ , respectively. These effects are associated with a large mass loss between 190°C and 420°C. This observed mass loss (40.1%) is correlated with the formation of  $\text{NiS}_2$  and a residue of six moles of carbon atoms per mole of initial complex (obs.: 43.3%; calc.: 44.6%).

Finally, the DSC curve shows a highly exothermic effect with a peak at 523°C. This effect is accompa-

nied by a large mass loss between 450°C and 620°C. The residue at 620°C, identified by X-ray diffraction is composed principally by NiO (obs.: 17.0%; calc.: 17.1%).

### 3.1.3. $[ZnCl(TzHy)_2]Cl$

The DSC curve shows an endothermic effect centered at 202°C which corresponds to the fusion of the complex. This is immediately followed by a decomposition centered at 252°C in the DSC curve, with a mass loss between 200°C and 440°C. The residue at 440°C is 58.0% of the initial sample. This value can be explained by the existence of one mole of  $ZnCl_2$  and six moles of carbon atoms per mole of initial complex (calc.: 56.2%).

Finally, from 440°C begins a slow combustion of carbonaceous residue and  $ZnCl_2$ , with a partial sublimation of  $ZnCl_2$  [5]. At the end of this process, the residue is ZnO as zincite, confirmed by X-ray diffraction (exp.: 13.4%).

### 3.1.4. $[Cd(TzHy)(\mu-Cl)_2]_n \cdot nH_2O$ .

The DSC curve shows a first endothermic effect centered at 130°C, which is associated with a mass loss of 6.1% between 70°C and 180°C. This effect can be attributed to the loss of crystallization water (Obs.: 6.1%; calc.: 5.7%). The calculated enthalpy to the dehydration is 251 J/g.

At 195°C begins a second effect centered at 213°C without mass loss. This effect corresponds to the fusion of the anhydrous complex. Immediately, occurs the decomposition of the anhydrous complex, characterized by an exothermic effect with three relative maxima at 222°C, 241°C and 265°C. This effect is accompanied with a strong mass loss between 195°C and 400°C. The residue obtained at 400°C has a mass of the 67.0% of initial mass. The composition of this residue may be formed for one or several species with total composition  $CdSCL$  and a carbonaceous mass corresponding at three moles of carbon atoms per mole of initial complex (cal.: 67.8%).

From 400°C begins a smooth mass loss, continued by a strong mass loss with a minimum at 760°C in the DTG curve. This effect is associated with a strong exothermic effect in the DSC curve. The residue at 810°C is CdS as greenockite, confirmed by X-ray diffraction.

The observed mass at 810°C (32.2%) is smaller than that calculated from the empirical formula (45.3%). This can be attributed to a partial sublimation of CdS [6].

## 3.2. IR spectra

The bands observed in the region 4000–150  $cm^{-1}$  and their assignments are summarized in Table 1.

### 3.2.1. $TzHyHCl$

*Vibrations of NH and  $NH^+$* : In the 3300–3000  $cm^{-1}$  range,  $TzHyHCl$  shows four strong bands at 3264, 3167, 3102 and 3013  $cm^{-1}$  which can be assigned to stretching vibrations of the NH and  $NH_2$  groups. Similar compounds show these vibrations in the same range [7]. The strong and sharp band recorded at 1604  $cm^{-1}$  is assigned to the  $\delta(NH_2)$  vibration [8]. At 1332 appears a band of medium intensity which can be assigned to  $\omega(CH_2)$ , whereas the two sharp bands at 1109 and 1062  $cm^{-1}$ , also of medium intensity, are assigned to  $r(NH_2)$  [9].

The  $\nu(NH^+)$  vibration is detected as two bands of medium intensity at 2823 and 2789  $cm^{-1}$ . Finally, the sharp band situated at 1541  $cm^{-1}$  has been attributed at  $\delta(NH^+)$  [10].

*Vibrations of  $CH_2$* : The bands of medium intensity in the 3000–2850  $cm^{-1}$  region are assigned to the stretching vibrations ( $\nu_a$  and  $\nu_s$ ) of  $CH_2$  [11]. The bending vibration,  $\delta(CH_2)$  is registered as two bands at 1452 and 1432  $cm^{-1}$  with low and medium intensity, respectively [10].  $\omega(CH_2)$  can be attributed at two bands with medium intensity at 1298 and 1251  $cm^{-1}$  [12]. The twisting vibration  $t(CH_2)$  is recorded at 1188 and 1136  $cm^{-1}$  with very low intensity [11]. The band of low intensity recorded at 859  $cm^{-1}$  can be assigned to the rocking vibration  $r(CH_2)$  [12].

*Vibrations of thiazoline ring*: The IR spectrum in the 4000–400  $cm^{-1}$  region shows the presence of characteristic bands due to the thiazoline ring at 1674  $cm^{-1}$  ( $W_1$ ), 982  $cm^{-1}$  ( $W_2$ ), 934  $cm^{-1}$  ( $W_3$ ), 785  $cm^{-1}$  ( $W_4$ ), 673  $cm^{-1}$  ( $W_5$ ), 630  $cm^{-1}$  ( $W_6$ ), 511  $cm^{-1}$  ( $W_7$ ), 596  $cm^{-1}$  ( $W_8$ ) and 427  $cm^{-1}$  ( $\Gamma_1$ ) [11].

*Vibration N–N*: The vibration  $\nu(N-N)$  can be assigned at one band of low intensity recorded at 1024  $cm^{-1}$ . This vibration is registered in the 1150–

Table 1  
Position ( $\text{cm}^{-1}$ ) and assignments of the bands of IR spectra

Assignment	TzHyHCl	Ni	Zn	Cd
$\nu(\text{H}_2\text{O})$		3392		3550 vs 3445 vs
	3264 vs	3260 vs	3288 vs	3284 vs
$\nu(\text{NH}_2)$	3167 vs	3191 vs	3235 vs	3207 vs
$\nu(\text{NH})$	3102 vs	3172 vs	3135 vs	3132 vs
	3013 vs		3099 vs	3035 vs
$\nu(\text{CH}_2)$	2981 m	2991 m	3004 m	2992 m
	2969 m	2944 m	2960 m	2962 m
	2908 m	2873 m	2866 m	2857 m
	2874 m			
$\nu(\text{NH}^+)$	2823 m			
	2789 m			
$W_1[\nu(\text{CN})]$	1674 vs	1645 vs	1646 vs	1651 vs
$\delta(\text{NH}_2)$	1604 vs	1595 vs	1579 vs	1605 vs
$\delta(\text{NH}^+)$	1541 m			
$\delta(\text{NH})$		1511 m	1527 w 1495 m	1537 w
$\delta(\text{CH}_2)$	1452 w	1468 vw	1450 vw	1458 vw
	1432 m	1429 vw	1434 vw	1441 vw
$\omega(\text{NH}_2)$	1332 m	1336 w	1351 w	1336 w
		1321 vw	1331 w	
$\omega(\text{CH}_2)$	1298 m	1279 vw	1281 m	1288 m
	1251 m	1258 w	1252 s	1258 s
$t(\text{CH}_2)$	1188 vw	1173 vs	1166 vs	1160 m
	1136 vw			1136 s
$r(\text{NH}_2)$	1109 m	1089 s	1086 s	1081 s
	1062 m			1026 sh
$\nu(\text{N-N})$	1024 w	1026 m	1034 vs	1014 vs
$W_2$	982 s	957 vw	954 w	951 w
$W_3$	934 s	869 vw		880 vw
$r(\text{CH}_2)$	859 w	837 vw	875 vw	
$W_4[\nu_a(\text{CS})]$	785 w	795 vw	823 vw	818 vw
$W_5[\nu_s(\text{CS})]$	673 s	674 m	673 w	665 m
$W_6$	630 s	617 w		
$W_8$	596 w		529 w	560 m
$W_7$	511 w	508 m	469 m	502 s
$\Gamma_1$	427 w	444 w	445 w	432 m
$\nu(\text{M-OH}_2)$		339 m		
$\nu(\text{M-N}_{\text{hydrazine}})$		299 m	329 m	346 m
$\nu(\text{M-Cl}_{\text{terminal}})$			275 s	
$\nu(\text{M-Cl}_{\text{bridge}})$				220 s
$\nu(\text{M-N}_{\text{thiazoline}})$				217 s
				211 s
$\nu(\text{M-Cl}_{\text{bridge}})$				179 m
				173 m
$\nu(\text{M-N}_{\text{thiazoline}})$		270 w	246 m 226 s	
Ligand	243 w			
	196 s	195 s		198 s
	171 s	168 s		163 s
	161 s		155 w	152 s

1025 cm<sup>-1</sup> region in the spectra of hydrazine [11], methylhydrazine [13], ethylhydrazine [13] and tetrafluorhydrazine [13], while is registered at more low frequencies (975–960 cm<sup>-1</sup>) in some hydrazinium salts [7].

### 3.2.2. Complexes

The bands assigned to  $\nu(\text{NH}^+)$  and  $\delta(\text{NH}^+)$  in the spectrum of TzHyCl are absent in the three complexes, which is according to the fact that the ligand acts in a deprotonated form. Moreover, the presence of water molecules in the Ni(II) and Cd(II) complexes is detected by bands due to the  $\nu(\text{H}_2\text{O})$  vibrations, registered in the 3550–3380 cm<sup>-1</sup> range.

In the low frequency region, all the complexes show bands assignable to metal-ligand stretching vibrations. Thus, the Ni(II) complex shows three bands due to such vibrations, which is concordant with the C<sub>i</sub> symmetry of the complex cation [3]. The band at 339 cm<sup>-1</sup> has been assigned to the  $\nu(\text{Ni}-\text{OH}_2)$  vibration, while the bands at 299 and 270 cm<sup>-1</sup> can be attributed to  $\nu(\text{Ni}-\text{N}_{\text{hydrazine}})$  and  $\nu(\text{Ni}-\text{N}_{\text{thiazoline}})$ , respectively [14,15]. In the spectrum of the Zn(II) complex, only four bands of the five predicted by the symmetry of the cation complex are detected [4]. Of these, the band at 329 cm<sup>-1</sup> is assigned to  $\nu(\text{Zn}-\text{N}_{\text{hydrazine}})$  [16], the band at 275 cm<sup>-1</sup> is assigned to  $\nu(\text{Zn}-\text{Cl})$  [17] and the bands registered at 246 and 226 cm<sup>-1</sup> are assignable to  $\nu(\text{Zn}-\text{N}_{\text{thiazoline}})$  [16]. According to the C<sub>i</sub> symmetry around the Cd centers, six bands are expected due to the Cd-ligand stretching vibrations, all of these have been registered in the spectrum. The band at 346 cm<sup>-1</sup> is assigned to  $\nu(\text{Cd}-\text{N}_{\text{hydrazine}})$  [14], the bands at 220, 217 and 211 cm<sup>-1</sup> include the  $\nu(\text{Cd}-\text{N}_{\text{thiazoline}})$  vibration [18] and two  $\nu(\text{Cd}-\text{Cl}_{\text{bridge}})$  vibrations [19], and the bands at 179 and 173 cm<sup>-1</sup> are also assignable to  $\nu(\text{Cd}-\text{Cl}_{\text{bridge}})$  vibrations [20].

### 3.3. UV-vis-NIR diffuse reflectance of $[\text{Ni}(\text{TzHy})_2(\text{H}_2\text{O})_2] \text{Cl}_2 \cdot 2\text{H}_2\text{O}$

The diffuse reflectance spectrum exhibits three zones of absorption assignable to d-d transitions: one multiplet of low intensity in the 10,500–13,250 cm<sup>-1</sup> range, one doublet at 17,300 and 18,000 cm<sup>-1</sup>, and another doublet at 26,800 and 28,800 cm<sup>-1</sup>, more intense. These bands may be assigned as  ${}^3\text{A}_{2g}(\text{F}) \rightarrow$

${}^3\text{T}_{2g}(\text{F}); {}^3\text{A}_{2g}(\text{F}) \rightarrow {}^1\text{E}_g; {}^3\text{A}_{2g}(\text{F}) \rightarrow {}^3\text{T}_{1g}(\text{F})$  and  ${}^3\text{A}_{2g}(\text{F}) \rightarrow {}^3\text{T}_{1g}(\text{P})$  transitions, respectively, in an idealized O<sub>h</sub> symmetry. The position of the observed spectral bands permits to calculate the ligand field parameters 10Dq and B, using the following known relationships [21]:

$$\begin{aligned} E[{}^3\text{T}_{2g}(\text{F}) \leftarrow \text{A}_{2g}(\text{F})] &= 10\text{Dq} \\ E[{}^3\text{T}_{1g}(\text{F}) \leftarrow {}^3\text{A}_{2g}(\text{F})] &= (1/2)(15\text{B} + 30\text{Dq}) \\ &\quad - (1/2)[(15\text{B} - 10\text{Dq})^2 \\ &\quad + 12\text{B} \cdot 10\text{Dq}]^{1/2} \\ E[{}^3\text{T}_{1g}(\text{P}) \leftarrow {}^3\text{A}_{2g}(\text{F})] &= (1/2)(15\text{B} + 30\text{Dq}) \\ &\quad + (1/2)[(15\text{B} - 10\text{Dq})^2 \\ &\quad + 12\text{B} \cdot 10\text{Dq}]^{1/2} \end{aligned}$$

The calculated values of the ligand field parameters 10Dq (11,350 cm<sup>-1</sup>) and B (764 cm<sup>-1</sup>) are consistent with the presence of a chromophore group [Ni<sup>II</sup>N<sub>4</sub>O<sub>2</sub>] [22].

## References

- [1] M. Gosálvez, C. Vivero, I. Álvarez, Biochem. Soc. Trans. 7 (1979) 191.
- [2] A. Brugarolas, M. Gosálvez, Lancet 68 (1979) 1.
- [3] A. Bernalte, M.A. Díaz, F.J.G. Barros, F.J. Higes, A.M. Pizarro, J. Romero, C. Valenzuela, Polyhedron 15 (1996) 1691.
- [4] A. Bernalte, M.A. Díaz, F.J.G. Barros, F.J. Higes, A.M. Pizarro, J.D. Martín-Ramos, C. Valenzuela, Polyhedron 16 (1997) 297.
- [5] B. De Castro, C. Freire, D. Domingues, J. Gomes, Polyhedron 10 (1991) 2541.
- [6] C. Duval, Inorganic Thermogravimetric Analysis, Elsevier, Amsterdam, 1953.
- [7] K.C. Patil, J.P. Vital, J.Chem.Soc., Dalton Trans. (1982) 2291.
- [8] D.N. Sathyanarayana, D. Nicholls, Spectrochim. Acta 34A (1978) 263.
- [9] K.C. Patil, R. Soundararajan, V.R.P. Verneker, Inorg. Chem. 18 (1979) 1969.
- [10] L.J. Bellamy, The Infrared Spectra of Complex Molecules, Chapman and Hall, London, 1975.
- [11] G. Mille, J.L. Meyer, J. Chouteau, J. Mol. Struct. 50 (1978) 247.
- [12] J.R. Durig, S. Richtmiller, Y.S. Li, J. Chem. Phys. 60 (1974) 253.
- [13] U. Anthoni, C. Larsen, P.H. Nielsen, Acta Chem. Scand. 22 (1968) 1025.

- [14] A.A. Rahman, M.P. Brown, M.M. Harding, C.E. Keggan, D. Nicholls, *Polyhedron* 7 (1988) 1147.
- [15] M. Nagase, Y. Yukawa, Y. Inomata, T. Takeuchi, *Bull. Chem. Soc. Jpn.* 62 (1989) 3247.
- [16] C. Preti, G. Tosi, *Can. J. Chem.* 54 (1976) 1558.
- [17] J.R. Ferraro, *Low-Frequency Vibrations of Inorganic and Coordination Compounds*, Plenum Press, New York, 1971.
- [18] A. Giusti, G. Peyronel, *Spectrochim. Acta* 38A (1982) 975.
- [19] G. Moggi, J.C. Bart, F. Cariati, R. Psaro, *Inorg. Chem. Acta* 60 (1982) 135.
- [20] F. Cariati, G. Ciani, L. Menabue, G.C. Pellacani, G. Rasu, A. Sironi, *Inorg. Chem.* 22 (1983) 1897.
- [21] A.B.P. Lever, *Inorganic Electronic Spectroscopy*, 2nd ed., Elsevier, Amsterdam, 1968, pp 420–511.
- [22] L. Sacconi, F. Mani, A. Bencini, in: G. Wilkinson (Ed.), *Comprehensive Coordination Chemistry*, Pergamon Press, New York, 1987, pp. 58–59.